Effects of Tat peptide on intracellular delivery of arsenic trioxide albumin microspheres

Jie Zhou[a], Qi-Hui Wang[b], Jin-Hua Liu[b] and Yan-Bin Wan[b]

The current study was designed to evaluate the ability of cell-penetrating peptides to deliver arsenic trioxide albumin microspheres (AsAMs) into bladder cancer cells. The transactivating transcriptional activator (Tat) peptide was labeled with the enhanced green fluorescent protein (EGFP) using eukaryotic vector construction and fusion gene expression techniques. Arsenic trioxide albumin mirospheres were prepared using the chemical crosslink and solidification method. The conjugate, Tat-EGFP-As_2O_3-AMs (TEAsAMs), was synthesized using the amine-reactive heterobifunctional linker agent *N*-succinimidyl-3-(2-pyridyldithio) propionate and verified by electrophoresis under reducing conditions and fluorescence microscopy. The intracellular delivery of TEAsAMs was evaluated by laser confocal microscopy and transmission electron microscopy. The arsenic content in the bladder cancer EJ cells was assayed to evaluate the efficiency of delivery. Gene sequencing showed that the pET-Tat-EGFP expression vector was constructed successfully. The expression of the Tat-EGFP fusion protein was verified by matrix-assisted laser desorption/ionization-time of flight analysis, and the protein was transduced into cell cytoplasm as observed under a fluorescence microscope. Electrophoresis under reducing conditions demonstrated the covalent linkage between Tat-EGFP and AsAMs. Under a laser confocal microscope and a transmission electron microscope, TEAsAMs surrounded by green fluorescence were shown to enter the cells faster than EGFP-As_2O_3-AMs, with an increase in the intracellular arsenic content being observed in cells treated with TEAsAMs compared with those treated with EGFP-As_2O_3-AMs. These results suggest that Tat peptide promotes the cellular uptake of large albumin microspheres with encapsulated arsenicals. *Anti-Cancer Drugs* 23:303–312 © 2012 Wolters Kluwer Health | Lippincott Williams & Wilkins.

Anti-Cancer Drugs 2012, **23**:303–312

Keywords: albumin microsphere, arsenic trioxide, cell-penetrating peptide

[a]College of Biomedical Engineering, South-Centeral University for Nationalities, Wuhan and [b]Department of Immunology, Guangxi Medical University, Nanning, China

Correspondence to Jie Zhou, College of Biomedical Engineering, South-Centeral University for Nationalities, Wuhan 430074, China
Tel: +86 27 67843221; fax: +86 27 67843221; e-mail: zhoujieuser@163.com

Received 20 May 2011 **Revised form accepted** 23 October 2011

Introduction

Bladder cancer is a type of significant and frequently occuring urinary system tumor. Some well-known chemotherapy drugs, such as mitomycin, pirarubicin, and hydroxy camptothecin, have little therapeutical effect. Moreover, these drugs might cause severe side effects. Arsenic trioxide (As_2O_3) is a toxic agent, but has been used as a traditional Chinese medicine for many years. Previous studies in our laboratory [1] and others [2] have shown that As_2O_3 inhibits the proliferation of bladder cancer cells. It triggers a highly regulated form of caspase-independent cell death through the mitochondrial death pathway [3,4]. But severe side effects might be caused after the instillation of As_2O_3 into the bladder of mice. The reason for this might be that As_2O_3 is absorbed into the blood circulation by the bladder mucous membrane. Therefore, we have prepared a sustained-release albumen microsphere dosage form of As_2O_3. Albumin microspheres are hollow biodegradable nanoparticles. When used as a vehicle, it may improve therapeutic effects and reduce side effects through a slow, controlled drug release mechanism [5]. We have synthetized slow-release arsenic trioxide albumin microspheres (AsAMs) using methods of chemical crosslinking and solidification [6]. Although the cell killing rate of AsAMs is higher after a 24-h exposure compared with an As_2O_3 solution, it is lower within the first 24 h, perhaps due to a low cellular penetration rate of the albumin microspheres in the early phase of the drug exposure. The reason for this might be that it is more difficult for AsAMs to enter the cancer cell and it might be discharged along with urine. Therefore, an increasing microsphere uptake into tumor cells is the key to improve the therapeutic effects of As_2O_3 in microspheres.

Cell-penetrating peptides (CPPs) are emerging as an attractive drug delivery tool because of their ability to translocate macromolecules across the cell membrane [7]. Among several CPPs, the transactivating transcriptional activator (Tat) peptide has been widely studied and is extensively used for drug delivery [8,9]. Tat is derived from the basic domain of HIV-1 Tat, which is rich in basic amino acids, and sufficient for intracellular transduction and subcellular localization [10]. In addition, this capacity for highly efficient translocation has been observed in a variety of cell lines with minimal toxicity, overcoming the challenge often faced with other delivery methods [11]. It has become evident that a single CPP may use multiple modes of cellular entry, depending on

0959-4973 © 2012 Wolters Kluwer Health | Lippincott Williams & Wilkins DOI: 10.1097/CAD.0b013e32834e75c1

the experimental conditions [12]. The modes of cellular entry are broadly categorized into two groups: energy-dependent endocytosis and energy-independent direct translocation across the membrane [13]. Nanoparticles that are chemically conjugated with Tat peptide can be efficiently delivered into mammalian cells [14–16] or across some body barriers of drugs, such as the blood–spinal cord barrier [17,18] and skin [19]. As a huge microparticle carrier, albumin microspheres are believed to be internalized mainly through endocytosis, especially macropinocytosis [20]. With superficial abundant amino groups, AsAMs could be linked with Tat peptide easily. Cellular uptake may be an issue for drug delivery, considering that the mean diameters of albumin microspheres, we have previously prepared are more than 2 μm [6]. Very few studies have shown that CPPs can promote the entry of large albumin microspheres into cancer cells. The objectives of this study were 2-fold to demonstrate and explore the possible mechanisms of cell permeation of Tat-peptide-coated AsAMs and to demonstrate that encapsulated arsenicals are delivered into bladder cancer cells and can be released slowly from microspheres. The enhanced green fluorescent protein (EGFP) was fused with Tat peptide to visualize albumin microspheres under a fluorescence microscope. The covalent bond between Tat peptide and microsphere was verified by electrophoresis under reducing conditions. Laser confocal microscopy and transmission electron microscopy were used to observe the intracellular delivery of Tat-EGFP-As_2O_3-AMs (TEAsAMs). The delivery efficiency of the encapsulated arsenicals was evaluated by measuring the arsenic content in the cells. If Tat peptide can promote the entry of albumin microsphere-encapsulated arsenicals into the bladder cancer cells, the therapeutic effect of arsenicals would increase. This would have an important application in the development of novel therapy for bladder cancer and other cancers as well.

Materials and methods

Materials

Escherichia coli BL21 (DE3), plasmid pEGFP-1, and pET30a were generous gifts from Dr Lan Xiuwan (Department of Biochemistry, Guangxi Medical University, Guangxi, China). BamHI, HindIII, T4DNA-joining enzyme, and the BAC protein assay kit were purchased from Fermentas China (Shenzheng, China). *N*-Succinimidyl-3-(2-pyridyldithio) propionate (SPDP), 1,4-dithiothreitol (DTT), isopropyl-β-D-thiogalactoside (IPTG), As_2O_3, Tween 80, and dialysis membrane were purchased from Sigma-Aldrich Chemicals (St. Louis, Missouri, USA). Ni-NTA His Resin was obtained from Qiagen (Hilden, German). Bovine serum albumin was procured from Sheng Ma Biotechnology Institute (Beijing, China). Fetal bovine serum (FBS) was procured from Invitrogen Corp (Eugene, Oregon, USA). The EJ human bladder cancer cell line was obtained from American Type Culture Collection (Rockville, Maryland, USA). EJ cells were grown in Roswell Park Memorial Institute medium (Sigma, St. Louis, Missouri, USA) supplemented with 10% FBS. All tissue culture media contained penicillin (5000 U/ml) and streptomycin (0.1 mg/ml). The cells were maintained at 37°C in the presence of 5% CO_2 in air. All the other chemicals used in this study were of analytical grade. The oligonucleotides encoding Tat peptide and EGFP primers were synthesized by Sangon Corporation (Shanghai, China).

Construction of expression vectors

The construction of the pET-Tat-EGFP expression vector was accomplished using a previously reported method [21], with minor modifications. In brief, the oligonucleotides, encoding the peptide containing 11 amino acids from the protein transduction domain of the HIV-1 Tat and EGFP sense primer, were synthesized. The sequences of the nucleotides were 5′-CG GGA TCC TAC GGT CGT AAG AAA CGT CGC CAG CGT CGC CGT ATG GTG AGC AAG GGC-3′. The sequences of the nucleotides encoding EGFP antisense primer were 5′-CGC AAG CTT CTT GTA CAG CTC GTC-3′. The Tat-EGFP fusion gene sequences were amplified using PCR from the pEGFP-1 plasmid. The PCR products and pET30a expression vector were digested with BamHI and HindIII. The digested fragments were joined with the T4DNA-joining enzyme, generating pET30a-Tat-EGFP. The sequences of Tat-EGFP were confirmed by sequencing analysis. To create Tat-lacking protein (EGFP alone), the EGFP gene was inserted in-frame BamHI/HindIII-cut pET30a to create the pET30a-EGFP vector. Gene sequencing was accomplished by Sangon Corporation.

Expression and purification of transactivating transcriptional activator-enhanced green fluorescent protein fusion protein

The expression constructs were transformed in *E. coli* BL21(DE3). Transformed bacteria were cultured in an LB broth medium containing 100 μg/ml of ampicillin at 37°C. Protein expression was induced by the addition of 1 mmol/l of IPTG (final concentration) at 37°C during the logarithmic growth phase. After a 5-h incubation, cells were harvested and lysed by BugBuster (Novagen, Darmstadt, Germany). The cell lysate containing Tat-EGFP fusion proteins with the His_6tag at their N termini was applied to Ni-NTA His Resin and washed with six bed volumes of binding buffer (pH 7.8) and four bed volumes of wash buffer (pH 6.0). Then, the binding protein was eluted with six bed volumes of imidazole wash buffer. Then, the protein solutions were captured and the target protein was concentrated by Millipore ultra-filtration dialysis. The protein concentrations were quantified using the BAC protein assay kit (Pierce, Rochford, Illinois, USA). The EGFP protein was expressed using the same methods. Protein sequencing was accomplished by Sangon Corporation using matrix-assisted laser desorption/ionization-time of flight analysis.

Penetration of the fusion protein into cells

EJ cells were obtained from American Type Culture Collection (Rockville, MD, USA) and were cultured in a phenol-red-free Roswell Park Memorial Institute-1640 medium containing 10% FBS, penicillin (5000 U/ml), and streptomycin (0.1 mg/ml) at 37°C in 5% CO_2. When the cells were 70% confluent, the culture medium was replaced with a fresh medium containing 10% FBS, and the EGFP or EGFP-Tat protein was added to the growth medium, at a final concentration of 4 μmol/l. All cells were divided into four groups, and treated at 5, 10, 20, or 30 min. The cells were then digested with 0.25% trypsin and washed with phosphate-buffered saline (PBS). The cell suspension was observed under a fluorescence microscope.

Preparation and characterization of arsenic trioxide albumin microspheres

AsAMs were prepared and characterized using the previously reported method [6]. In brief, As_2O_3 (2 g) was dissolved in PBS solution (70 ml) and sodium hydroxide was added to promote dissolution. The pH was adjusted to 7.4 to prepare an As_2O_3 stock solution (100 ml, 20 mg/ml, pH 7.4). Bovine serum albumin (450 mg) was dissolved in the As_2O_3 stock solution (1.5 ml) and then mixed with injection oil (60 ml). The mixture was dispersed at a high speed (9000 rpm) for 60 s. Arachis oil (180 ml) was then added and the mixture was stirred (300 r/min) for 2 h, whereas the glutaric dialdehyde solution (25%, 1.5 ml) was added slowly. Then, diethyl ether (120 ml) was added, and after 0.5 h, the mixture was centrifuged (5000 rpm, 20 min). The precipitate was washed with acetone (200 ml) three times. The product was resuspended in acetone (10 ml) and was filtered through a filter membrane (5-μm aperture). The filtrate was dried and resuspended, and the resultant AsAMs were aliquoted and stored in desiccated containers until use.

A scanning electron microscope (SEM) was used to determine the morphology of AsAMs. The samples for SEM analysis were prepared by suspending 1 mg of AsAMs in 1 ml of DH_2O. Then, 200 μl of the suspended AsAMs were transferred onto a stub, dehydrated, and sputter coated with silver/palladium for further analysis [22]. Dynamic laser light scattering was used to further quantify the size of the AsAMs. The nanoparticle sample was prepared by suspending 1 mg of NPs in 10 ml of 1 × PBS. The suspended NPs were set for 1 min to remove any large aggregates. Then, samples were decanted into a glass scintillation vial. A dynamic laser light scattering system (Brookhaven Instruments BI-200SM; Brookhaven Instruments Corporation, Holtville, New York, USA) calculated the nanoparticle diameter by the regularized non-negatively constrained least squares method. The range of nanoparticle size was reported as differential distribution values [22].

Preparation of Tat-EGFP-As_2O_3-AMs

Tat-EGFP fusion proteins were conjugated to AsAMs using SPDP conjugation methods as described previously in our studies for antibody conjugation to AsAMs [2]. In the initial step, purified Tat-EGFP fusion protein (0.4 mg) was mixed with SPDP (40 μg) for 30 min, and excess SPDP was removed by dialysis in acetate buffer (0.01 mol/l acetate, pH 4.5). DTT (15.4 mg) was added and the mixture was stirred lightly for 30 min. Protein peak Tat-EGFP-SH was collected. AsAMs (5 mg) were suspended in acetate buffer, SPDP (250 μl), and stirred for 30 min. The precipitate (AsAMs-PDP) was centrifuged (5000 rpm, 10 min) and washed with PBS three times. After Tat-EGFP-SH and AsAMs-PDP were mixed and shaken for 15 h at 4°C, the TEAsAMs produced were collected by centrifugation (5000 rpm,10 min) and washed with PBS three times and frozen in desiccated containers (−20°C). EGFP (0.4 mg) was used to prepare EGFP-As_2O_3-AMs (EAsAMs) according to the same methods as described above.

Characterization of Tat-EGFP-As_2O_3-AMs

TEAsAMs (5 mg) or EAsAMs (5 mg) were suspended in PBS (1 ml) and then hydrolyzed by pepsin. The arsenic content loaded in TEAsAMs or EAsAMs was measured using an atomic spectrofluorometer (AFS-2202; Beijng Haiguang Equipment Company, Beijing, China) [23]. The drug loading of TEAsAMs and EAsAMs was calculated as the total mass of loaded arsenic divided by the total mass of polymer expressed as a percentage. The encapsulation efficiency of TEAsAMs and EAsAMs was calculated as the experimentally measured loading divided by the theoretical loading expressed as a percentage.

The rate of arsenic release from TEAsAMs was determined in PBS solution (pH = 7.4) at 37°C using membrane dialysis according to the described methods [22]. In brief, 3 mg of TEAsAMs were added to 2 ml of PBS and the mixture was sonicated for 20 s to disperse the particles. The nanoparticle suspension was then placed in a Pierce dialysis tube with a molecular weight cutoff at 10,000 Da, and the tube was subsequently immersed in fresh PBS (20 ml) and incubated at 37°C on a rotary shaker (100 rpm for 5 days). The liquid medium was completely replaced with fresh PBS (37°C) daily. The amount of arsenic released was measured as above.

The covalent bond between Tat-EGFP and AsAMs was identified indirectly by electrophoresis under reducing conditions [1]. TEAsAMs (10 μl, 5 mg/ml) were mixed with the electrophoresis buffer (10 μl) containing 2 μl of DTT (15.4 mg/ml). TEAsAMs added to electrophoresis buffer without DTT were used as a control and the blank group was Tat-EGFP. The samples were separated at 75 V for 1.5 h and 150 V for 2 h. The gel was then stained with polyacrylamide gel electrophoresis dyeing solution (1.25 g

of Coomassie brilliant blue, 500 ml of methanol, 100 ml of glacial acetic acid, and 400 ml of distilled water) for 30 min. For evaluation of its integrity, TEAsAMs (200 μg) were dissolved in PBS and washed with Hank's buffer three times, and then observed under a fluorescence microscope (Nikon Corporation, Tokyo, Japan), with EAsAMs as a control.

Analysis of intracellular delivery

The intracellular delivery of TEAsAMs was determined using a laser confocal microscope. EJ cells were cultured as above until the cells were 70% confluent. After culture with TEAsAMs for 3 h, the cells were then digested with 0.25% trypsin and washed with a fresh medium three times and observed under a laser confocal microscope. The control group was EJ cells treated with EAsAMs.

A transmission electron microscope (1200-EX II, JEOL Inc., Akishima, Japan) was used to observe the intracellular delivery and analyze the mechanism of action. EJ cells were treated with TEAsAMs or EAsAMs for 6 h. The sample was placed in plastic capsules filled with resin, hardened at 60°C for 24 h, and then sectioned into 0.6-μm thickness with a glass knife. For TEM imaging, the block was trimmed down to the area of interest and sectioned into 0.1-μm thickness with a diamond knife. All the samples were viewed at an accelerating voltage of 75 kV.

Analysis of arsenic by atomic spectrofluorimetry

EJ cells (1 ml; 1×10^6) were treated with 1 ml of TEAsAMs (128.8 μg/ml of arsenic) for 0.5, 1, 2, 4, 8, 16, or 24 h at 37°C in the presence of 10% FBS at the same arsenic concentration as EAsAMs or As_2O_3 solutions as controls. After washing with PBS three times, the cells were digested and centrifuged (5000 rpm for 3 min) and washed an additional three times. After treating with concentrated nitric acid and perchloric acid, the solution was reduced with ascorbic acid and thiourea. The solution was suspended in PBS (1 ml) and the arsenic content was measured using an atomic spectrofluorometer (AFS-2202, Beijng Haiguang Equipment Company) [23]. Assays were performed in quadruplicate.

Statistical analysis

The arsenic contents were expressed as μg/ml. All results were presented as mean ± standard error. Statistical significance was determined using analysis of variance. *P* values of less than 0.05 were considered statistically significant.

Results

Construction and expression of transactivating transcriptional activator-enhanced green fluorescent protein fusion protein

The PCR amplification products of Tat-EGFP and EGFP genes are shown in Fig. 1a, which are consistent with the

Fig. 1

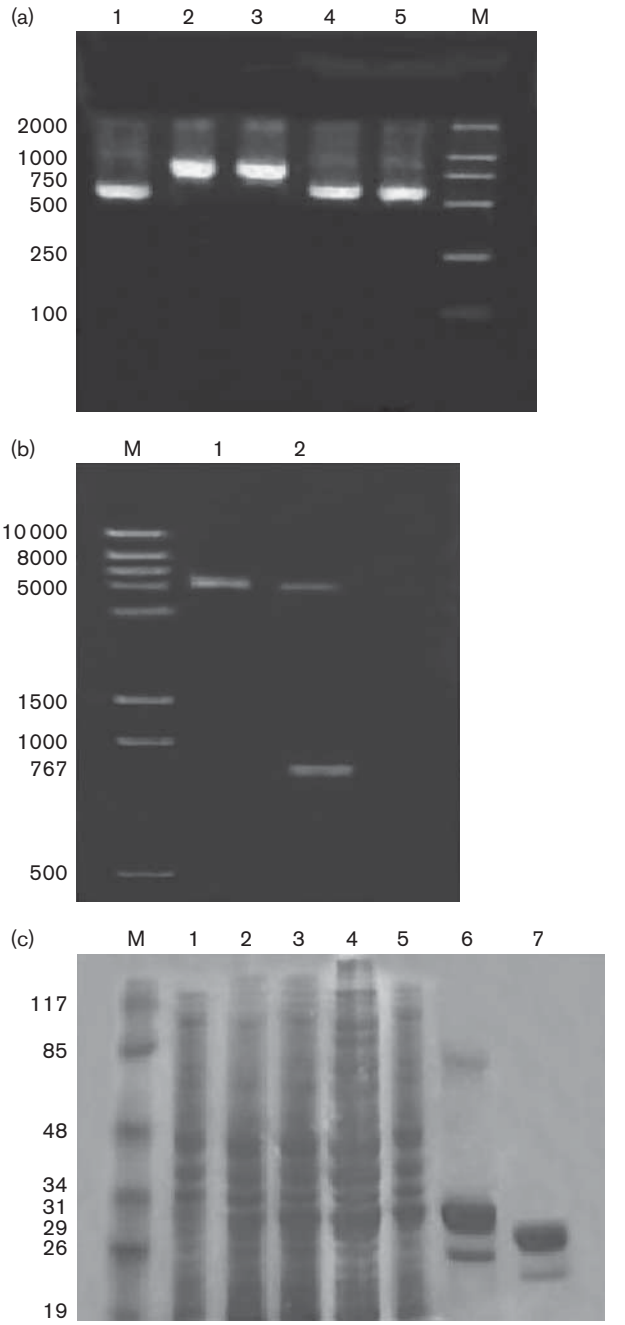

Construction of pET30a-transactivating transcriptional activator (Tat)-enhanced green fluorescent protein (EGFP) vector and expressions of Tat-EGFP fusion protein. (a) PCR amplification product of Tat-EGFP and EGFP. Lanes 1, 4, and 5: EGFP PCR products (734 bp). Lanes 2 and 3: Tat-EGFP PCR products (767 bp). M, DNA marker. (b) Identification of pET30a-Tat-EGFP plasmid digested by HindIII and BamHI. M. DNA marker. Lane 1: pET30a/BamHI + HindIII (5400 bp). lane 2: pET30a-Tat-EGFP/BamHI + HindIII showed two straps (5400 bp, 767 bp). (c) Expression of EGFP and Tat-EGFP fusion protein analyzed by SDS-polyacrylamide gel electrophoresis. M. protein molecular weight marker. Lane 1: *Escherichia coli* lysate. Lane 2: transformed *E. coli* lysate without IPTG. Lane 3: *E. coli* lysate with IPTG. Lane 4: sediment of transformed *E. coli* lysate. Lane 5: supernatant of transformed *E. coli* lysate. Lane 6: purtified Tat-EGFP. Lane 7: purtified EGFP.

Fig. 2

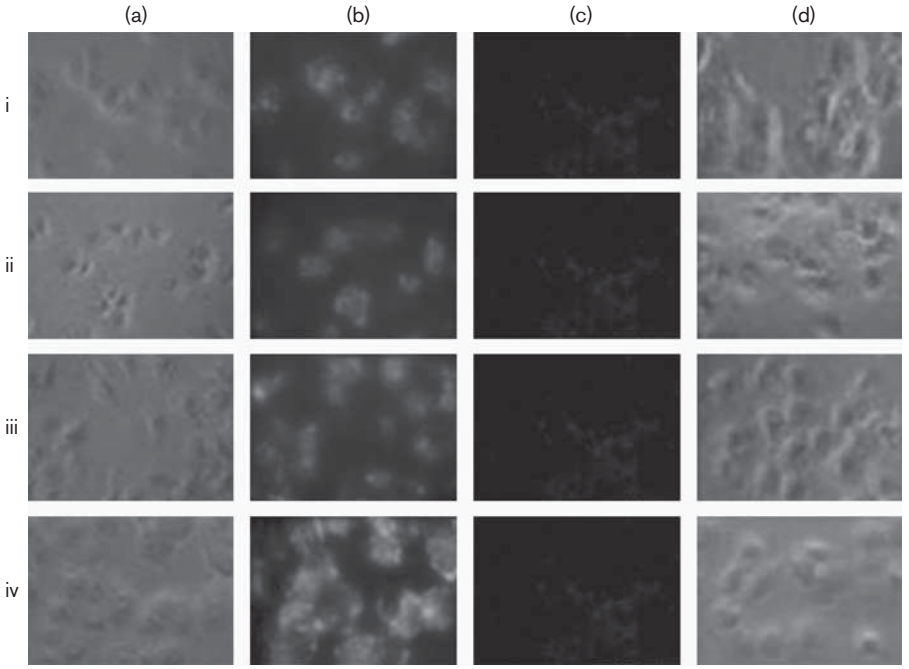

Observation of the penetrating activity of transactivating transcriptional activator (Tat)-enhanced green fluorescent protein (EGFP) and EGFP protein in EJ cells, i: 5 min after Tat-EGFP or EGFP protein was added to a final concentration of 4 μm/l; ii: 10 min after Tat-EGFP or EGFP protein was added; iii: 20 min after TAT-EGFP or EGFP protein was added; and iv: 30 min after Tat-EGFP or EGFP protein was added. The samples were observed using a light and fluorescence microscope at × 400 magnification. (a) EJ cell treated with Tat-EGFP under a microscope. (b) EJ cell treated with Tat-EGFP under a fluorescence microscope. (c) EJ cell treated with EGFP under a microscope. (d) EJ cell treated with EGFP under a fluorescence microscope. Green fluorescence showing the Tat-EGFP fusion protein.

predicted size on the basis of their gene sequences. Recombinant plasmid pET30a-Tat-EGFP was constructed successfully (Fig. 1b), showing that the sequence of amplified fragment was inserted into pET30a expression plasmid accurately. Gene sequencing verified the correct sequence of the constructed expression plasmid. *E. coli* BL21 (DE3) transformed with Tat-EGFP and EGFP expressed the fusion proteins well, with IPTG induction. In addition, the fusion protein expression could be easily monitored during the entire expression and purification process due to their green fluorescence. SDS-polyacrylamide gel electrophoresis analysis demonstrated purified Tat-EGFP and EGFP proteins at the expected sizes (Fig. 1c). The purity of the Tat-EGFP protein was about 90%, and the concentration of protein in solution was 1.24 mg/ml.

Transduction and intercellular localization of the transactivating transcriptional activator-enhanced green fluorescent protein fusion proteins in EJ cells

As shown in Fig. 2, green fluorescence appeared in EJ cells, indicating that the Tat-EGFP fusion protein was delivered into the cells. Moreover, the fluorescence intensity increased gradually with the duration of exposure. However, hardly any green fluorescence was detected in the control EGFP group. The green fluorescence localization was observed to be within the cytoplasm.

Characterization of arsenic trioxide albumin microspheres

Under scanning electron microscopy, the majority of AsAMs were spherical in shape with a narrow particle size (see Fig. 3a for SEM of AsAMs). The grain sizes were between 1 and 3 μm.

Characterization of Tat-EGFP-As_2O_3-AMs

The loading of arsenic in TEAsAMs was 8.34 ± 2.2% (w/w, 100 mg of TEAsAMs contained 8.34 mg of arsenic), with an encapsulation efficiency of 91.32 ± 12.1%. The loading of arsenic in EAsAMs was 8.81 ± 2.5% (w/w), with an encapsulation efficiency of 92.12 ± 10.6%. The analysis of the release of the encapsulated arsenic from the TEAsAMs indicated that about 90% of arsenic was released from TEAsAMs over a period of 5 days under in-vitro incubation in PBS (see Fig. 3b). The cumulative release percentage increased rapidly in the arsenic solution group, with 91.34% of the arsenic released within the first day and approximately 99% within the first 3 days. However, the cumulative release percentage increased slowly for the TEAsAMs and EAsAMs groups,

Fig. 3

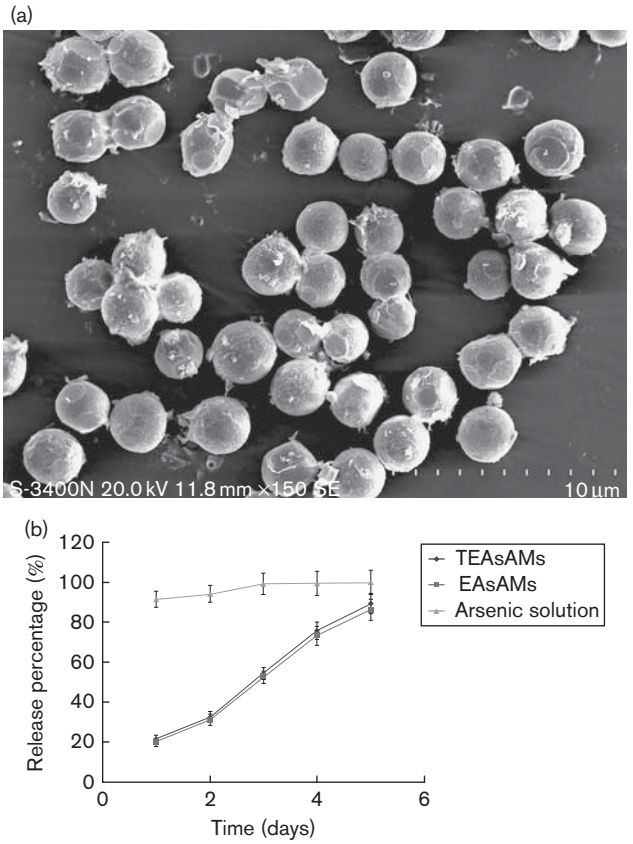

Characteristics of Tat-EGFP-As_2O_3-AMs (TEAsAMs). (a) 5000 × standard error of the mean image of AsAMs. Scale bar is 10 µm. (b) Cumulative release percentage of arsenic from TEAsAMs, EGFP-As_2O_3-AMs (EAsAMs), or arsenic solution after incubation in phosphate-buffered saline at 37°C for 5 days. Data are represented as mean ± standard error ($n = 5$). The *y*-axis shows the release percentage; the *x*-axis shows the time in days.

Fig. 4

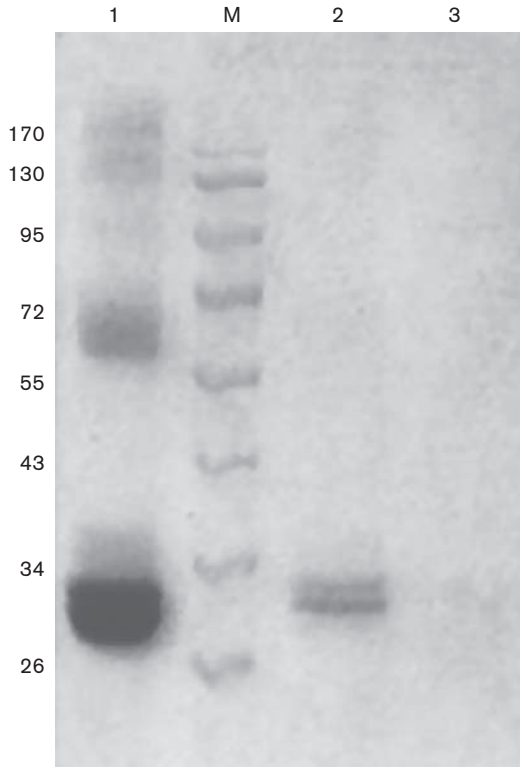

Electrophoresis under reducing conditions of transactivating transcriptional activator (Tat)-enhanced green fluorescent protein (EGFP)-As_2O_3-AMs (TEAsAMs). M: protein marker; lane 1: Tat-EGFP fusion protein group; lane 2: TEAsAMs + 1,4-dithiothreitol group; lane 3: arsenic trioxide albumin microspheres + 1,4-dithiothreitol group.

with the release percentages being 89.23 ± 5.12 and 86.11 ± 5.32% on the fifth day (Fig. 3b), respectively.

The TEAsAMs groups treated with DTT showed protein bands at the distal end. At the same level, the Tat-EGFP groups had one similar protein strap, which was coincident with the molecular weight of Tat-EGFP protein (Fig. 4), indicating that the Tat-EGFP protein bond was broken from the microspheres. No protein band was found in the control group, indicating that Tat-EGFP peptide had not been disintegrated from the microspheres and therefore could not enter the glue, and confirming that the bond between Tat-EGFP and the microspheres was not ionic.

Under a fluorescence microscope, many green fluorescent spots could be observed, which showed that TEAsAMs were surrounded by multiple Tat-EGFP peptides. Similar green fluorescent spots were found in the EAsAMs groups (Fig. 5a).

Intracellular delivery of Tat-EGFP-As_2O_3-AMs

Under a laser confocal microscope, many green fluorescent spots were observed in EJ cells treated with TEAsAMs, indicating that TEAsAMs entered into the cells (Fig. 5b). However, hardly any green fluorescent spots were observed in cells treated with EAsAMs (Fig. 5b).

Under a transmission electron microscope, cells treated with TEAsAMs had many phagocytotic vesicles, indicating that TEAsAMs entered cells by endocytosis. Hardly any phagocytotic vesicles were found in EJ cells treated with EAsAMs (Fig. 6a, b and c).

Arsenic content in bladder cancer cells

Figure 6d shows the arsenic contents (mean ± standard error) at different times after EJ cells were treated with various drug preparations over a 24-h period. Within the first 4 h of incubation, there was a slight increase in the average arsenic content of the TEAsAMs groups, reaching a 3.15-fold higher level than that in the EAsAMs groups at 2 h. After 4 h, the content decreased gradually. This might be due to some arsenic in EJ being released gradually into

Fig. 5

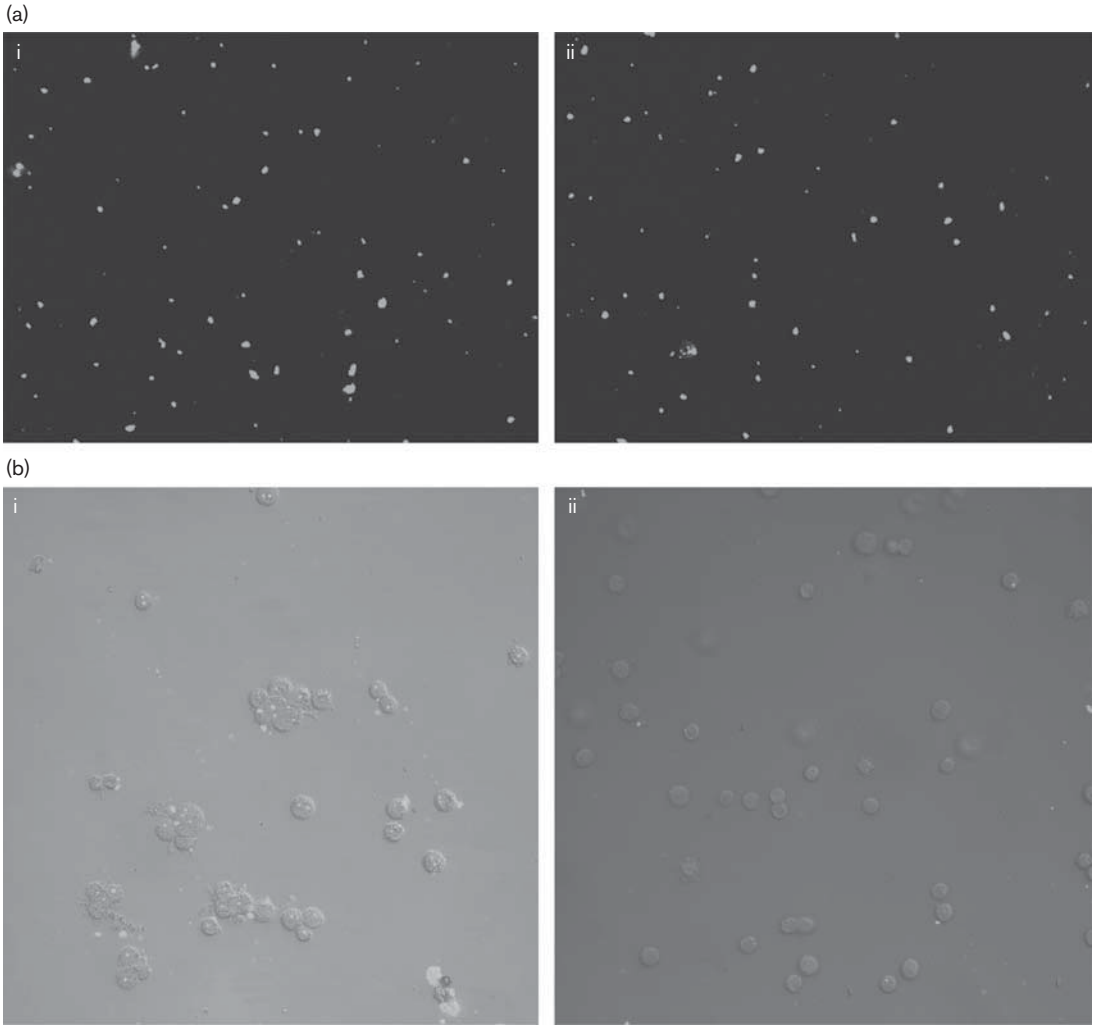

(a) Fluorescence microscope observation of transactivating transcriptional activator (Tat)-enhanced green fluorescent protein (EGFP)-As_2O_3-AMs (TEAsAMs) and EGFP-As_2O_3-AMs (EAsAMs). i: TEAsAMs under a microscope at × 400 magnification; ii: EAsAMs under a microscope at × 400 magnification. Green fluorescent spots demonstrate the EGFP peptide. (b) Laser confocal micrography of the intracellular delivery of TEAsAMs and EAsAMs. i: EJ cell treated with TEAsAMs under a microscope at × 200 magnification; ii: EJ cell treated with EAsAMs under a microscope at × 200 magnification. Green fluorescent spots demonstrate the Tat-EGFP-conjugated AsAMs.

the culture solution, as more cells died with time. The EAsAMs group had a lower average arsenic content compared with the TEAsAMs group ($P < 0.01$). The mean arsenic content of the arsenic solution group peaked at 0.5 h and decreased gradually. This group had lower concentrations than those found in the TEAsAMs group (3.76 ± 0.31 vs. 5.23 ± 0.57) at 2 h and the EAsAMs group (2.1 ± 0.23 vs. 2.33 ± 0.19) at 8 h.

Discussion

CPPs have been identified in HIV-1 TAT, antennapedia protein, and HSV-1 VP22 [24]. They can display functions as carriers for the efficient delivery of proteins that do not permeate living cells [25]. Although the mechanism of CPPs uptake across the plasma membrane remains elusive, these CPPs have successfully delivered proteins, nucleic acids, small molecule therapeutics, quantum dots, and MRI contrast agents, among other things [12]. It has been suggested that various properties of peptides, such as molecule length and charge delocalization, as well as the properties of the drugs/molecules to be delivered, such as size and charge, can have a significant impact on the mechanism of peptide uptake [26]. Successful delivery of nanoparticles into cells by CPPs has been reported [27]. Macropinocytosis has been reported as the major route of internalization of cationic CPPs [28,29], especially for large Tat-fusion proteins (in excess of 30 kDa). Other endocytotic pathways including clathrin-dependent and caveolin-dependent endocytosis [30,31] and trans-Golgi network-mediated internalization [32] have been described

for CPPs. Moreover, different mechanisms of membrane translocation and endocytosis may occur simultaneously for most of CPPs. Cellular uptake of biologically active Pep-1 or MPG/cargo complexes is directly correlated with the structure of the nanoparticle that creates a local high concentration of peptides at the cell surface [33,34].

Recently, it has been reported that CPPs might promote the entry of nanoparticles into cells. Murakami *et al.* [14] used TAT peptide to promote the intracellular delivery of doxorubicin by genetically engineered high-density lipoprotein nanoparticles, resulting in enhanced growth inhibition of cancer cells *in vitro* and tumor *in vivo*. Using a murine xenograph model of human glioma, Niu *et al.* [35] revealed that the fusion peptide p14ARF-TAT was a promising approach for tumor growth suppression when combined with efficient targeting. The particle sizes of the methoxy polyethylene glycol/poly epsilon-caprolactone diblock copolymers were about 40 and 60 nm. When conjugated with a Tat analog through an ester or a disulfide linkage, it can transfect pCMV-Luc into COS7 cells, suggesting that it can be used as a safe and efficient systemic nonviral gene vector [15]. Bionanocapsule (BNC) is a hollow nanoparticle composed of the L-protein of the hepatitis B virus surface antigen, which can deliver genes or drugs into specific human hepatocytes [16]. Altering the specificity of BNCs by genetically introducing CPPs, such as arginine-rich peptides into BNCs, can lead to efficient internalization of the CPP-fused BNC into various types of cells [16]. It has been suggested that CPPs facilitate the passage of nanoparticles through some body barriers of drugs, protein, and genes, such as the blood–spinal cord barrier [17,18] and skin layers [19], and reach the site of action. Therefore, nanoparticles linked to CPPs may represent a promising carrier to deliver therapeutic macromolecular agents across the body barrier and penetrate into the effect site.

Albumin microspheres are a type of hollow biodegradable nanospheres several micrometers in diameter. With a slow-release property, albumin nanospheres represent an attractive dosage form for the delivery of anticancer drugs [5,36,37]. To increase the therapeutic effect of

Fig. 6

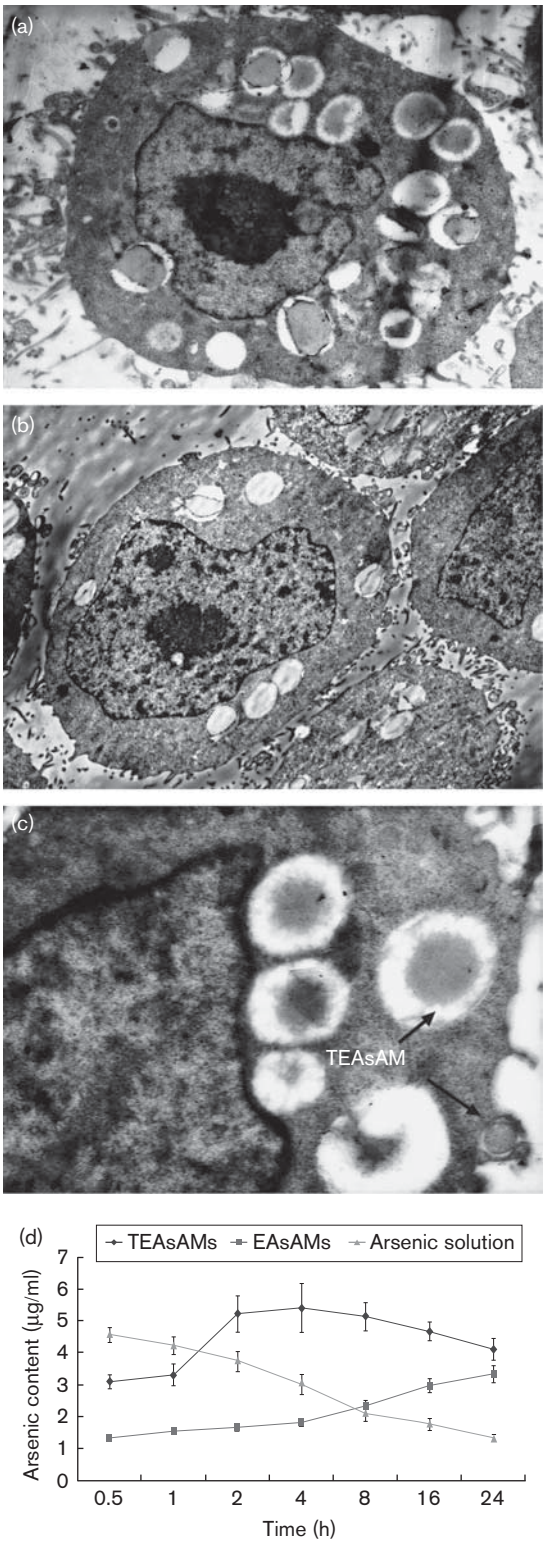

Fig. 6

Observation of the intracellular delivery of transactivating transcriptional activator (Tat)-enhanced green fluorescent protein (EGFP)-As_2O_3-AMs (TEAsAMs) and EGFP-As_2O_3-AMs (EAsAMs) in EJ cells (a) EJ cell treated with TEAsAMs under a transmission electron microscope at $\times$3800 magnification. (b) EJ cell treated with EAsAMs under a transmission electron microscope at $\times$3800 magnification (c) EJ cell treated with TEAsAMs under a transmission electron microscope at $\times$4500 magnification. The black arrowhead shows TEAsAMs that have undergone endocytosis. The smaller TEAsAMs were undergoing endocytosis. (d) Variance of the arsenic content (mean $\pm$ standard error) at different times after EJ cells were treated with drug TEAsAMs; arsenic content after EJ cells were treated with TEAsAMs. EAsAMs, arsenic content after EJ cells were treated with TEAsAMs. Arsenic solution, arsenic content after EJ cells were treated with As_2O_3 solution. *y*-axis shows the average number of arsenic content (error bars are standard error); the *x*-axis shows the time in hours.

As_2O_3 and decrease the toxic effect, we have prepared AsAMs. To increase the drug-loading rate to reach the effective cell-killing dose, AsAMs about 2 μm in size were prepared. To determine the therapeutic effects *in vivo*, AsAMs were irrigated into a mouse bladder at different time points (data not shown). Although the growth of the bladder tumor was inhibited, the therapeutic effects were not as good as predicted (data not shown). The reason could be that AsAMs were egested along with urination and the action time of AsAMs was not long enough. To further improve the therapeutic effects, in the present study, we used Tat peptide to promote the entry of AsAMs into the bladder cancer cells.

DTT, a reducing agent, can open disulfide bonds between peptides. In the present study, after the treatment with DTT, TEAsAMs were broken into a protein strap corresponding to the molecular weight of Tat-EGFP, suggesting that Tat-EGFP and AsAMs were linked covalently using the SPDP conjugation method. Under a fluorescence microscope, TEAsAMs were shown to be surrounded by green fluorescence, indicating that AsAMs could be conjugated with multiple Tat-EGFPs, creating a local high concentration of peptides on the cell surface.

Compared with the EAsAMs group, green fluorescence was seen in EJ cells treated with TEAsAMs group under a laser confocal microscope, suggesting that the conjugated-Tat peptide could promote the intercellular transfer of TEAsAMs. Then, we used a transmission electron microscope to observe EJ cells after treatment with TEAsAMs or EAsAMs for 6 h. These results showed that some EAsAMs entered into EJ cells by endocytosis. However, the quantity was less than that with TEAsAMs. These results also indicated that Tat peptide enhanced the intercellular permeation of TEAsAMs.

In the present study, the arsenic content in EJ cells treated with TEAsAMs was higher than that with EAsAMs, indicating that the encapsulated arsenicals were delivered into EJ cells faster than EAsAMs. However, the arsenic content in EJ cells treated with TEAsAMs is lower than the arsenic solution group at the beginning and increased gradually with time, showing that arsenic in TEAsAMs enters cells slower than arsenic in solution.

It has been shown that Tat peptide can facilitate the passage of microspheres larger than 2 μm through the cell membrane, and encapsulated arsenicals enter cells at the same time. The conjugate dosage promotes increased transport efficiency of the carrier-drug microspheres. Two chemotherapy advantages of the microspheres may be realized simultaneously, including its use as a slow-release drug and promotion of drug entry into cells. Future studies should determine whether or not TEAsAMs have better therapeutic effects than EAsAMs *in vitro* and *in vivo*.

Conclusion

Our studies indicate that Tat peptide enhances intercellular permeation of TEAsAMs by translocating microspheres across the cell membrane. CPPs can be used to transport the encapsulated arsenicals payloads into bladder cancer cells, and the arsenical is released slowly from these microspheres. This method may be applicable for the delivery of other anticancer drugs.

Acknowledgements

The authors thank Dr Lan Xiuwan for his assistance with the protocols in molecular biology and conjugation chemistry and Dr Kong Xiaolong for his assistance with the albumin microsphere preparation technique. They also thank Dr Li Weidong for his assistance with microscopic techniques. The study was supported by the National Natural Science Foundation of China (Grant numbers 30700836 and 81160314) and China Postdoctoral Science Foundation projects (Grant numbers 20070420152 and 200801268).

Conflicts of interest

There are no conflicts of interest.

References

1 Zhou J, Zeng FQ, Li C, Tong QS, Gao X, Xie SS, *et al.* Preparation of arsenic trioxide-loaded albuminutes immuno-nanospheres and its specific killing effect on bladder cancer cell *in vitro*. *Chin Med J* 2005; **118**:50–55.
2 Wang Y, An R, Dong X, Pan S, Duan G, Sun X. Protein kinase C is involved in arsenic trioxide-induced apoptosis and inhibition of proliferation in human bladder cancer cells. *Urol Int* 2009; **82**:214–221.
3 Scholz C, Wieder T, Stärck L, Essmann F, Schulze-Osthoff K, Dörken B, *et al.* Arsenic trioxide triggers a regulated form of caspase-independent necrotic cell death via the mitochondrial death pathway. *Oncogene* 2005; **24**: 1904–1913.
4 Jutooru I, Chadalapaka G, Sreevalsan S, Lei P, Barhoumi R, Burghardt R, *et al.* Arsenic trioxide downregulates specificity protein (Sp) transcription factors and inhibits bladder cancer cell and tumor growth. *Exp Cell Res* 2010; **316**:2174–2188.
5 Jones AK, Bejugam NK, Nettey H, Addo R, D'Souza MJ. Spray-dried doxorubicin-albumin microparticulate systems for treatment of multidrug resistant melanomas. *J Drug Target* 2010 [Epub ahead of print].
6 Zhou J, Zeng F, Xiang G, Xie S, Wei S. Preparation of arsenic trioxide albumin microspheres and its release characteristics *in vitro*. *J Huazhong Univ Sci Technolog Med Sci* 2005; **25**:310–319.
7 Heitz F, Morris MC, Divita G. Twenty years of cell-penetrating peptides: from molecular mechanisms to therapeutics. *Br J Pharmacol* 2009; **157**:195–206.
8 Rapoport M, Lorberboum-Galski H. TAT-based drug delivery system: new directions in protein delivery for new hopes? *Expert Opin Drug Deliv* 2009; **6**:453–463.
9 Zhao JF, Chen JY, Mi L, Wang PN, Peng Q. Enhancement of intracellular delivery of anti-cancer drugs by the Tat peptide. *Ultrastruct Pathol* 2011; **35**:119–123.
10 Zaro JL, Vekich JE, Tran T, Shen WC. Nuclear localization of cell-penetrating peptides is dependent on endocytosis rather than cytosolic delivery in CHO cells. *Mol Pharm* 2009; **6**:337–344.
11 Nagahara H, Vocero-Akbani AM, Snyder EL, Ho A, Latham DG, Lissy NA, *et al.* Transduction of full-length TAT fusion proteins into mammalian cells: TAT-p27Kip1 induces cell migration. *Nat Med* 1998; **4**:1449–1452.
12 Fonseca SB, Pereira MP, Kelley SO. Recent advances in the use of cell-penetrating peptides for medical and biological applications. *Adv Drug Deliv Rev* 2009; **61**:953–964.
13 Vivès E, Richard JP, Rispal C, Lebleu B. TAT peptide internalization: seeking the mechanism of entry. *Curr Protein Pept Sci* 2003; **4**: 125–132.

14 Murakami T, Wijagkanalan W, Hashida M, Tsuchida K. Intracellular drug delivery by genetically engineered high-density lipoprotein nanoparticles. *Nanomedicine (Lond)* 2010; **5**:867–879.
15 Tanaka K, Kanazawa T, Shibata Y, Suda Y, Fukuda T, Takashima Y, *et al*. Development of cell-penetrating peptide-modified MPEG-PCL diblock copolymeric nanoparticles for systemic gene delivery. *Int J Pharm* 2010; **396**:229–238.
16 Shishido T, Yonezawa D, Iwata K, Tanaka T, Ogino C, Fukuda H, *et al*. Construction of arginine-rich peptide displaying bionanocapsules. *Bioorg Med Chem Lett* 2009; **19**:1473–1476.
17 Wang H, Zhang S, Liao Z, Wang C, Liu Y, Feng S, *et al*. PEGlated magnetic polymeric liposome anchored with TAT for delivery of drugs across the blood–spinal cord barrier. *Biomaterials* 2010; **31**:6589–6596.
18 Rao KS, Reddy MK, Horning JL, Labhasetwar V. TAT-conjugated nanoparticles for the CNS delivery of anti-HIV drugs. *Biomaterials* 2008; **29**:4429–4438.
19 Patlolla RR, Desai PR, Belay K, Singh MS. Translocation of cell penetrating peptide engrafted nanoparticles across skin layers. *Biomaterials* 2010; **31**:5598–5607.
20 El-Andaloussi S, Johansson HJ, Holm T, Langel U. A novel cell-penetrating peptide, M918, for efficient delivery of proteins and peptide nucleic acids. *Mol Ther* 2007; **15**:1820–1826.
21 Mie M, Takahashi F, Funabashi H, Yanagida Y, Aizawa M, Kobatake E. Intracellular delivery of antibodies using TAT fusion protein A. *Biochem Biophys Res Commun* 2003; **310**:730–734.
22 Hindi KM, Ditto AJ, Panzner MJ, Medvetz DA, Han DS, Hovis CE, *et al*. The antimicrobial efficacy of sustained release silver-carbene complex-loaded L-tyrosine polyphosphate nanoparticles: characterization, in-vitro and in-vivo studies. *Biomaterials* 2009; **30**:3771–3779.
23 Yang GF, Li XH, Zhao Z, Wang WB. Preparation, characterization, in-vivo and in-vitro studies of arsenic trioxide Mg-Fe ferrite magnetic nanoparticles. *Acta Pharmacol Sin* 2009; **30**:1688–1693.
24 Gupta B, Levchenko TS, Torchilin VP. Intracellular delivery of large molecules and small particles by cell-penetrating proteins and peptides. *Adv Drug Deliv Rev* 2005; **57**:637–651.
25 Chugh A, Eudes F, Shim YS. Cell-penetrating peptides: nanocarrier for macromolecule delivery in living cells. *IUBMB Life* 2010; **62**:183–193.
26 Mueller J, Kretzschmar I, Volkmer R, Boisguerin P. Comparison of cellular uptake using 22 CPPs in 4 different cell lines. *Bioconjug Chem* 2008; **19**:2363–2374.
27 Sawant R, Torchilin V. Intracellular delivery of nanoparticles with CPPs. *Methods Mol Biol* 2011; **683**:431–451.
28 Wadia JS, Stan RV, Dowdy SF. Transducible TAT-HA fusogenic peptide enhances escape of TAT-fusion proteins after lipid raft macropinocytosis. *Nat Med* 2004; **10**:310–315.
29 Kaplan IM, Wadia JS, Dowdy SF. Cationic TAT peptide transduction domain enters cells by macropinocytosis. *J Control Release* 2005; **102**:247–253.
30 Richard JP, Melikov K, Brooks H, Prevot P, Lebleu B, Chernomordik V. Cellular uptake of unconjugated TAT peptide involves clathrin-dependent endocytosis and heparan sulfate receptors. *J Biol Chem* 2005; **280**:15300–15306.
31 Ziegler A, Nervi P, Dürrenberger M, Seelig J. The cationic cell-penetrating peptide CPP(TAT) derived from the HIV-1 protein TAT is rapidly transported into living fibroblasts: optical, biophysical and metabolic evidence. *Biochemistry* 2005; **44**:138–148.
32 Fischer R, Fotin-Mleczek M, Hufnagel H, Brock R. Break on through to the other side-biophysics and cell biology shed light on cell-penetrating peptides. *Chembiochem* 2005; **6**:2126–2142.
33 Gros E, Deshayes S, Morris MC, Aldrian-Herrada G, Depollier J, Heitz F, *et al*. A non-covalent peptide-based strategy for protein and peptide nucleic acid delivery. *Biochim Biophys Acta* 2006; **1758**:384–393.
34 Munoz-Morris MA, Heitz F, Divita G, Morris MC. The peptide carrier Pep-1 forms biologically efficient nanoparticle complexes. *Biochem Biophys Res Commun* 2007; **355**:877–882.
35 Niu G, Driessen WH, Sullivan SM, Hughes JA. In-vivo anti-tumor effect of expressing p14ARF-TAT using a FGF2-targeted cationic lipid vector. *Pharm Res* 2011; **28**:720–730.
36 Grinberg O, Gedanken A, Patra CR, Patra S, Mukherjee P, Mukhopadhyay D. Sonochemically prepared BSA microspheres containing gemcitabine, and their potential application in renal cancer therapeutics. *Acta Biomater* 2009; **5**:3031–3037.
37 Bozdağ S, Capan Y, Vural I, Dalkara T, Dogan AL, Guc D. In-vitro cytotoxicity of mitoxantrone-incorporated albumin microspheres on acute promyelocytic leukaemia cells. *J Microencapsul* 2004; **21**:751–760.